Thesis

T-box Transcription Factor *BRACHYURY* and *SOX2* Increase Self-Renewal and Invasive Phenotype in Adenoid Cystic Carcinoma: Implication for a New Therapeutic Principle

Koudai Nakamura

Supervisor: Professor Dr. Tsuyoshi Sugiura

Department of Maxillofacial Diagnostic and Surgical Science,

Field of Oral and Maxillofacial Rehabilitation,

Graduate school of Medical and Dental Sciences,

Kagoshima University

Abbreviations

EMT	Epithelial–mesenchymal transition
CSCs	Cancer stem cells
shRNA	Small hairpin RNA
GFP	Green fluorescence protein
EDTA	Ethylendiaminetetraacetic acid
ACC	adenoid cystic carcinoma
cDNA	complementary DNA
DMEM	Dulbecco’s modified Eagle’s medium
EGF	epidermal growth factor
FBS	fetal bovine serum
FGF	fibroblast growth factor
PBS	phosphate-buffered saline

Index

Abstract

Background: The high frequencies of recurrence and distant metastasis of adenoid cystic carcinoma (ACC) emphasize the need to better understand the biological factors associated with these outcomes. Recent studies suggest that epithelial–mesenchymal transition (EMT) correlates with cancer metastasis. In addition, there is growing evidence of the association of EMT with cancer stem cells (CSCs). Recently, we showed that the T-box transcription factor *BRACHYURY* could be a strong regulator of EMT. Further, we previously established the metastatic ACCS-M GFP cell line and reported that *SOX2* knockdown partially inhibits EMT phenotypes of ACCS-M GFP cells. Thus, in this study, we further tested whether *BRACHYURY* and *SOX2* is a regulator of cancer stemness by means of forced expression and silencing of these genes in adenoid cystic carcinoma (ACC) cell lines.

Methods: *BRACHYURY*, *SOX2*, or both were transfected into ACC cell lines. Short hairpin RNA (shRNA) silencing of these genes was also performed. We analysed these cell lines with respect to self-renewal phenotypes using a sphere-formation assay, and we assessed the expression levels of EMT markers and stem cell markers using real-time reverse transcription-polymerase chain reaction (RT-PCR). Cell migration and invasiveness in vitro were evaluated using a wound healing assay and a tumor cell dissemination assay, respectively. Characteristics of CSCs were also analyzed by sphere-forming ability and *in vivo* tumorigenicity.

Results: Forced expression of *BRACHYURY* or *SOX2* slightly increased expression of EMT and stem cell markers and the self-renewal phenotype. The expression levels, however, were much lower compared to those of cancer stem cell-like cells. Forced co-expression of *BRACHYURY* and *SOX2* strongly upregulated EMT and stem cell markers and the self-renewal phenotype. Cell migration and invasiveness in vitro were also remarkably enhanced. These synergistic effects increased expression levels of *FIBRONECTIN*, *SNAIL*, *SLUG*, *ZEB1*, and *TGF-β2*. In particular, the effects on *FIBRONECTIN* and *TGF-β2* were significant. *BRACHYURY* knockdown significantly inhibited cell migration and invasion, and decreased tumorigenicity in ACC cells.

Conclusions: We found that *BRACHYURY* and *SOX2* synergistically promote cancer stemness in

ACC cells. This finding points to the importance of gene or protein networks associated with *BRACHYURY* and *SOX2* in the development and maintenance of the CSC phenotype. This study demonstrates that *BRACHYURY* knockdown reduces invasiveness of CSCs *in vivo*, suggesting that *BRACHYURY* silencing may be a useful therapeutic tool for salivary gland carcinoma including adenoid cystic carcinoma.

Keywords: *BRACHYURY*; *SOX2*; Epithelial–Mesenchymal transition (EMT); cancer stem cell (CSC); Adenoid cystic carcinoma (ACC)

Introduction

Metastasis is a multistep cascade involving the migration of tumor cells from their site of origin, evasion from host defence systems, subsequent seeding at distant organs, and growth of secondary tumors. Recent studies have revealed that a specific change in the cancer cell phenotype, epithelial–mesenchymal transition (EMT), is involved in the metastasis mechanism. Accumulating evidence supports the importance of EMT in cancer progression and metastasis in several types of cancer: head and neck, breast, lung, and prostate cancer [1–4]. We also previously reported clinical evidence that EMT strongly correlates with poor prognosis in patients with oral squamous cell carcinoma [5]. In order to spawn macroscopic metastases, which are often facilitated by EMT, disseminated cancer cells presumably need a self-renewal ability similar to that exhibited by stem cells. From this point of view, the EMT process, which allows for migration and metastasis of cancer cells, would be also the key of a self-renewal capability to disseminated cancer cells. Actually, the accumulated evidences of relationship between EMT and cancer stem cells (CSCs) was reported recently [3,6–10]. The EMT or CSC program appears to be controlled by genes normally expressed in early embryos, including *TWIST, SNAIL, SLUG, ZEB1, and SOX2* [11–14]. These genes encode the transcription factors which enables the tumor cells to migrate and invade like mesenchymal cells. CSCs were proved to be resistant to chemotherapy and radiotherapy [15, 16], and CSCs should be the real target for the future new concept of cancer therapies [17, 18].

The T-box transcription factor *BRACHYURY* has been reported as a key gene for mesoderm formation during embryonic stage [19]. Recently, *BRACHYURY* is also recognised to induce EMT in human carcinoma cell lines [20]. In our previous study, we demonstrated that a CSC-like cell line (adenoid cystic carcinoma), ACCS-M GFP undergoes EMT. [21] This finding suggests that EMT may be directly linked to CSCs, and that

BRACHYURY controls EMT and the CSC phenotype (cancer stemness). We also confirmed that expression of Brachyury protein strongly correlates with EMT and poor prognosis in oral cancer patients [5].

In this regard, *BRACHYURY* silencing could effectively control cancer stemness and offer a new concept for the development of cancer treatments. In this study, we used forced expression and silencing of *BRACHYURY* and *SOX2* in adenoid cystic carcinoma cell lines to confirm that *BRACHYURY* and *SOX2* are regulators of the CSC phenotype.

Materials and Methods

1. Cells and Culture

ACCS (human oral adenoid cystic carcinoma cell lines), ACCS GFP, and ACCS-M GFP were established and reported previously in our laboratory [21]. In brief, ACCS-GFP was established from the parental cell line ACCS by transfecting green fluorescence protein (GFP) gene. These cell lines had similar morphological characteristics, growth rates, and tumorigenicity in vitro and in vivo. Tumorigenicity of ACCS-GFP was similar to the parental ACCS, (22.2% incidence). ACCS-GFP cells were injected to the tongues of nude mice and the developed tumor was clearly detectable with green fluorescence under excitation light. ACCS-M GFP cell line was established by in vivo selection process repeatedly. ACCS-M GFP cells exhibited high tumorigenicity (100% incidence) and spontaneous metastases to submandibular lymph nodes (100% incidence) [21].

Colony selection after individual transfection procedure was performed using resistance to neomycin (G418; Sigma-Aldrich; St. Louis, MO, USA). The cell lines were maintained in Dulbecco's modified Eagle medium (DMEM; Sigma-Aldrich, St. Lois, MO, USA) supplemented with 10% fetal bovine serum (FBS; ICN Biomedicals; Aurora, OH, USA), 2 mM L-glutamine, penicillin G, and streptomycin in a humidified incubator with an atmosphere of 5% CO_2 at 37 °C.

2. Transfection and Knockdown of BRACHYURY and SOX2. Real-Time RT-PCR

Real-time RT-PCR was employed to quantify the mRNA expression levels of the indicated EMT-related genes, embryonic stem cell markers, and differentiation markers in ACC cells. Total RNA was extracted and purified using TRIzol Reagent (Invitrogen). The first-strand cDNA synthesis and amplification of target mRNA for quantification were performed using a real-time PCR system: LightCycler FastStart DNA Master SYBER Green 1 kit (Roche Diagnostics; Mannheim, Germany). The mRNA levels were quantified in triplicate. The

PCR cycling conditions are as follows; 10 min at 95 °C for 1 cycle followed by 45 cycles at 95 °C for 30 s, 60 °C for 30 s, and 72 °C for 60 s. Dissociation curve analysis, normalisation by β-actin mRNA levels and quantification of target mRNA expression level were analysed using the LightCycler 2.0 System software package (Roche Applied Science; Indianapolis, IN, USA). The specific primers for EMT, stem cell markers, and differentiation markers are shown in Table 1. All primers were purchased from NIHON Gene Research Laboratories, Inc. (Sendai, Japan).

Table 1. Primers used in real-time RT-PCR.

Gene (human)	Primer Sequence	
E-CADHERIN	(F) 5' CAA CTG GAC CAT TCA GTA CAA C 3'	(R) 5' TCC ATG AGC TTG AGA TTG AT 3'
CLAUDIN	(F) 5' GAC AAC ATT CAC TGCC TCA GG 3'	(R) 5' TTC ACA TTT GGT GAT TCT CG 3'
OCCULUDIN	(F) 5' CTC GAA GAA AGA TGG ACA GGT 3'	(R) 5' GCC ATG GGA CTG TCA ACT C 3'
ZO-1	(F) 5' CGA AGG AGT TGA GCA GGA AAT CT 3'	(R) 5' TCC ACA GGC TTC AGG AAC TTG 3'
DESMOPLAKIN	(F) 5' ACC GCT GGC AAA GGA TAG AT 3'	(R) 5' CCA CTT GCA GAA AGC CTG AT 3'
VIMENTIN	(F) 5' ATT CAC TCC CTC TGG TTG ATA C 3'	(R) 5' CGT GAT GCT GAG AAG TTT CG 3'
N-CADHERIN	(F) 5' GAC AAC ATT CAC TGC TCA GG 3'	(R) 5' TTC ACA TTT GGT GAT TCT CG 3'
FIBRONECTIN 1	(F) 5' CAA TGC CAG GAT TCA GAG AC 3'	(R) 5' CTT CGA CAG GAC CAC TTG AG 3'
SNAIL	(F) 5' TCC ACA AGC ACCAAG AGT C 3'	(R) 5' ATG GCA GTG AGA AGG ATG TG 3'
SLUG	(F) 5' ACT GCT CCA AAA CCT TCT CC 3'	(R) 5' TGG TCA GCA CAG GAG AAA ATG 3'
TWIST 1	(F) 5' CTC AGC TAC GCC TTC TCG 3'	(R) 5' ACT GTC CAT TTT CTC ATT CTC TG 3'
TWIST 2	(F) 5' AGG AGC TCG AGA GGC AG 3'	(R) 5' CGT TGA GCG ACT GGC TG 3'
ZEB1	(F) 5' CTC ACA CTC TGG GTC TTA TTC TC 3'	(R) 5' GTC TTC ATC CTC TTC CCT TGT C 3'
ZEB2	(F) 5' AAA GGA GAA AGT ACC AGC GG 3'	(R) 5' AGG AGT CGG AGT CTG TCA TAT C 3'
TGFB2	(F) 5' TTA ACA TCT CCA ACC CAG CG 3'	(R) 5' TCC TGT CTTTAT GGT GAAGCC 3'
GSK3B	(F) 5' GGT CTA TCT TAA TCT GGT GCT GG 3'	(R) 5' AGG TTC TGC GGT TTA ATA TCC C 3'
NODAL	(F) 5' ACC CAG CTG TGT GTA CTC AA 3'	(R) 5' TGG TAA CGT TTC AGC AGA C 3'
4-Oct	(F) 5' TAT CGA GAA CCG AGT GAG AG 3'	(R) 5' TCG TTG TGC ATA GTC GCT 3'
PAX6	(F) 5' GGC GGA GTT ATG TAT ACC TAC 3'	(R) 5' CTT GGC CAG TAT TGA GAC AT 3'
REX1	(F) 5' AAA CGG GCA AAG ACA AGA 3'	(R) 5' GCT CAT AGC ACA CAT AGC CAT 3'
LEFTY	(F) 5' TGT ATC CAT TGA GCC CTC T 3'	(R) 5' CAG GAA ATG GAA GGA CAC A 3'
NANOG	(F) 5' ACC CAG CTG TGT GTA CTC AA 3'	(R) 5' GCG TCA CCA TTG CTA TT 3'
BRACHYURY	(F) 5' TGC TGC AAT CCC ATG ACA 3'	(R) 5' CGT TGC TCA CAG ACC ACA 3'
SOX2	(F) 5' TGG GTT CGG TGG TCA AGT 3'	(R) 5' CTC TGG TAG TGCTGG GAC A3'
AFP	(F) 5' CTG CAA ACT GAC CAC GCT 3'	(R) 5' TGA GAC AGC AAG CTG AGG AT 3'

4. The Sphere-Formation Assay

Cultured cells were recovered and plated for floating cultures at a density of 5×10^4 cells/mL

in 60-mm non-coated dishes with serum-free DMEM containing basic fibroblast growth factor (bFGF, 40 ng/mL) and epidermal growth factor (EGF, 20 ng/mL). The cells were incubated in a humidified atmosphere at 37 °C and 5% CO_2, and bFGF and EGF were added to the medium every other day during culture period. After 10 days, the diameters of each cell sphere were measured, and the numbers of sphere with a diameter >100 μm were counted as primary spheres. For passaging of the primary spheres, the spheres were collected by centrifuge and treated with 0.05% trypsin/0.02% ethylendiaminetetraacetic acid (EDTA) and dissociated into single cells. The dissociated cells were plated to 24-well culture plates at a density of 10^4 cells/mL in a serum-free medium and allowed to grow for further 10 days in a serum-free medium to obtain secondary spheres.

5. The Wound Healing Assay

Cancer cells were plated at the density of 6×10^5 cells per well in a 6-well plate (BD Falcon) in DMEM with 10% FBS and allowed to attach for 24 h to obtain confluent monolayer of cells. Then monolayer cells were treated with 25μg/ml of Mitomycin C for 25min at 37°C to prevent cell growth. The confluent monolayer of cells is scratched to make wounds using a plastic pipette tip (200 μL), and the cells were washed with phosphate-buffered saline (PBS) and arrowed to migrate for 24 h. Randomly chosen wound fields were photographed under a fluorescence microscope (BZ-8000; Keyence; Osaka, Japan) every 8 h for 24 h. The wound areas were analysed using the following formula:

Wound area (%) = (wound area after the indicated period / initial wound area) × 100

6. Evaluation of Tumor Dissemination from the Primary Cancer Nest

Evaluation of tumor dissemination from a primary cancer nest was performed as described previously [22]. One million cells were pelleted and resuspended in 25 μL of DMEM and 25 μL of type I collagen (AteloCell; IAC-30; Koken; Tokyo, Japan) to form a solid cell cluster. The collagen-embedded tumor cell pellets were incubated to solidify for 30 min at 37 °C in a

1.5-mL microcentrifuge tube. Five hundred microliters of type I collagen containing fibroblasts (10^5 cells/mL) were added to a 6-well plate (BD Falcon, Franklin Lakes NJ, USA). The collagen-embedded tumor cells were embedded in the collagen-embedded fibroblasts and incubated to solidify for 30 min at 37°C. DMEM was added on top of the collagen gels, and the incubation was continued. After 7 days of culture, tumor migration was observed as green fluorescence under a fluorescence microscope (BZ-8000; Keyence, Japan). Cancer cell invasiveness was evaluated by tumor dissemination from the tumor cell pellet (mimics a primary tumor nest). Evaluation were made by measuring the distance of all cells from the edge of the nest in 5 randomly selected standardised rectangular light fields (500 × 100 μm), and the values were summed (invasion value, Supplemental Figure 1.).

7. MTT assay

The ACCS cell lines were seeded into CellTiter 96 Aqueous Non-radioactive Cell Proliferation Assay G4000 plates (Promega, Madison, WI, USA) at a density of 5×10^3 cells per well and incubated in DMEM containing 10% FBS for 8 h in a humidified incubator under an atmosphere of 5% CO_2 at 37°C. After incubation, ACCS cells were analyzed by CellTiter 96 Aqueous Non-radioactive Cell Proliferation Assay G4000 (Promega) according to the manufacturer's instructions. The absorbance of samples at 590 nm (A590) was measured with a microplate reader (Model 680, Bio-Rad, USA). All experiments were carried out in triplicate and repeated 3 times.

Data were normalized to the untreated controls and reported as % viability. The concentration-viability curve was generated using a non-linear regression model with the Solver function of Microsoft Excel.

8. ACCS metastatic orthotopic implantation mouse model

The animal experimental protocols were approved by the Animal Care and Use Committee of Kagoshima University and Kyushu University. Eight-week-old female athymic nude mice

(BALBcAJcl-nu) were purchased from Kyudo (Fukuoka, Japan). The mice were housed in laminar flow cabinets under specific pathogen-free conditions in facilities. For the experimental metastasis studies, 1×10^6 cells in 40 μL phosphate- buffered saline (PBS) were injected into the tongue using a syringe with a 27-gauge disposable needle (TOP Plastic Syringe, Tokyo, Japan) under intraperitoneal diethyl ether anesthesia. The primary tumor volumes were measured weekly, calculated as length× width × thickness, and mice were sacrificed when the primary tumor volume reached 100 mm^3. After sacrifice, tumors of the tongue and metastases, from tongue tumor in cervical lymph nodes, lungs, and liver were visualized macroscopically under light excitation. After visualization, the primary tumors and metastatic sites were examined pathologically and immunohistochemically.

9. Statistical Analysis

All data were calculated as mean ± SD and processed using analysis of variance (ANOVA) for multiple group comparison. When ANOVA is significant, two groups comparison using the Student's t-test is performed. Statistical analyses were calculated by means of the statistical software SPSS 13.0. Statistical significance was assumed at $P < 0.05$.

Results

1. Forced Expression of BRACHYURY does not Promote Self-Renewal Capacity, but a BRACHYURY Knockdown Suppresses the Self-Renewal Capacity in Adenoid Cystic Carcinoma Lines

We previously reported successful isolation of highly metastatic and tumorigenic CSC-like cells-the ACCS-M GFP cell line-from non-metastatic (0% incidence) and low tumorigenic (22.2% incidence) parental adenoid cystic carcinoma ACCS GFP cells using in vivo selection [21]. Because the accumulated evidences of relationship between metastasis and CSCs has been reported, therefore, in the present study, we tested the hypothesis that Brachyury can promote CSC features in adenoid cystic carcinoma cells. For this purpose, we established stable Brachyury transfectants of ACCS-GFP and ACCS-Bra cell lines. We also confirmed the effect of a Brachyury knockdown on ACCS-M GFP cells by means of Brachyury shRNA (Figure 1A). Forced expression of *BRACHYURY* slightly increased (2.0-fold) sphere formation (the number of spheres) in the primary sphere assay in comparison to parental ACCS-GFP cells (P = 0.0983, ANOVA), but had no effect in the secondary sphere assay (P = 0.125, ANOVA). In contrast, the Brachyury knockdown on ACCS-M GFP cells remarkably inhibited sphere formation in both the primary (P = 0.0001, ANOVA) and the secondary assay (P = 0.0001, ANOVA), with respect to both the diameter and the number of spheres (Figure 1).

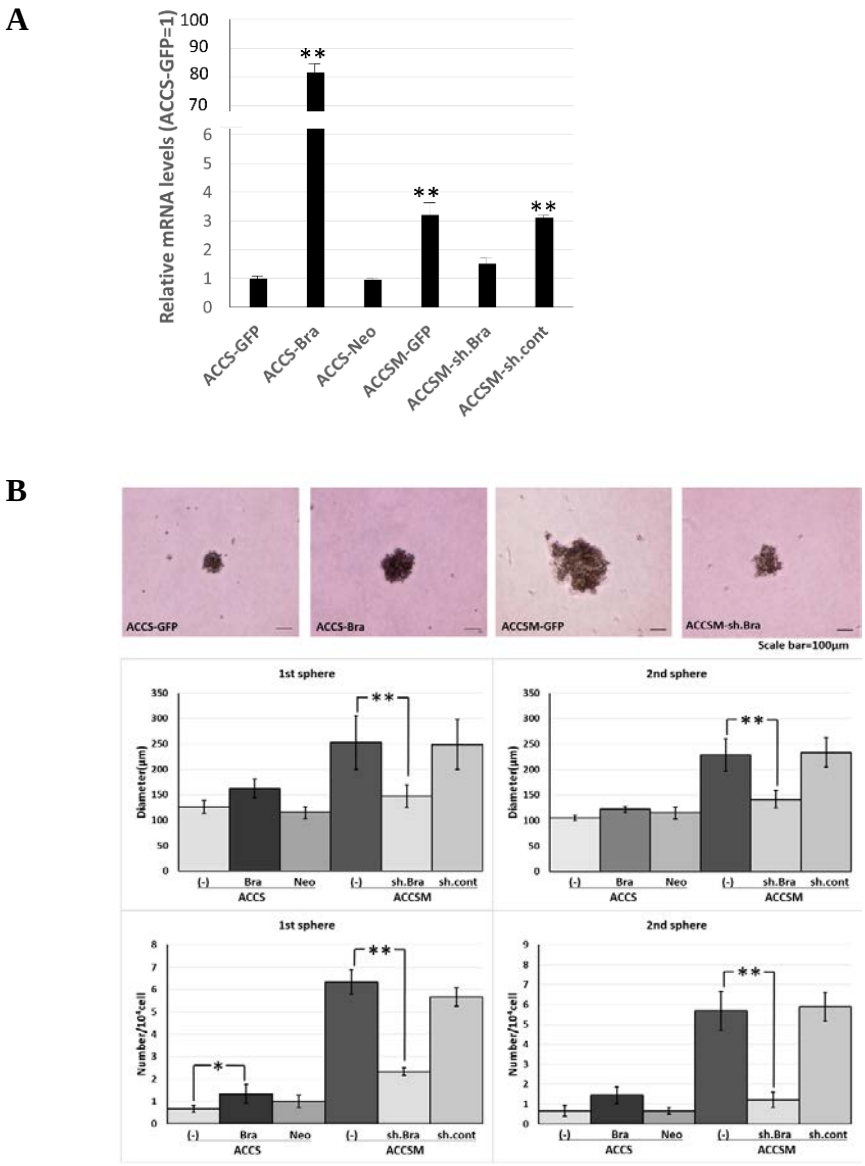

Figure 1. Effects of *BRACHYURY* transfection on the sphere-forming ability of ACCS (adenoid cystic carcinoma) cells.

Brachyury mRNA expression levels of the indicated ACCS (adenoid cystic carcinoma) cells and in derivative clones [ACCS-Brachyury (Bra), ACCS-Neomycin (Neo), ACCSM-sh.Brachyury (sh.Bra), and ACCSM-sh.control (sh.cont)] were quantified using real-time RT-PCR. mRNA level was compared with that in ACCS-GFP cells (parental cell line), and the data are shown in arbitrary units as relative mRNA levels (ACCS-GFP = 1.0) (**A**). ACCS cells were cultured at a density of 5×10^4 cells/mL in a serum-free medium for floating culture for 10 days (primary spheres). Primary spheres (day 10) were dissociated into individual cells and further cultured at a density of 10^4 cells/mL for 10 days. The spheres were observed under a phase contrast microscope (**B**, top panel). Sphere diameters were measured (**B**, middle panel), and numbers (diameter >100 μm) (**B**, bottom panel) were counted. Sphere numbers were standardised as a sphere number per 10^4 cells originally seeded (**B**, bottom panel). The experiments were performed in triplicate, and the data were calculated as mean ± SD. Statistical significance of differences was analysed using the Student's t test. * $P < 0.05$, ** $P < 0.01$.

2. Forced Expression of BRACHYURY Weakly Induces EMT-Related Markers and Stem Cell Markers in Adenoid Cystic Carcinoma Cell Lines

We next analysed the effect of *BRACHYURY* expression on EMT-related markers and stem cell markers in ACCS (Figure 2) and cell lines. EMT and CSC markers were evaluated their expression level using quantitative real-time RT-PCR (Figure 3). Each mRNA level was compared with that in the parental cells, ACCS GFP cells, and the data are shown as relative mRNA levels (ACCS GFP levels are set to 1.0 arbitrary unit). We analysed the expression levels of EMT-related genes (Figures 2A), stem cell markers (Figure 2B), and differentiation markers (Figures 2C). In ACCS cells, forced expression of *BRACHYURY* increased expression of *CLAUDIN*, *OCCULUDIN*, *VIMENTIN*, *FIBRONECTIN*, *SLUG*, *ZEB1*, *GSK3β*, *OCT4*, and *NANOG* and caused a decrease in *E-CADHERIN* expression. These changes were similar to the changes observed in the CSC-like cell line ACCS-M GFP in all markers, but the changes were smaller in *BRACHYURY* transfectants (except for *CLAUDIN*, *OCCLUDIN*, and *NANOG*). In contrast, mRNA levels of all markers decreased significantly in the *BRACHYURY* knockdown cells (ACCS-M shBra) compared to parental ACCS-M GFP cells.

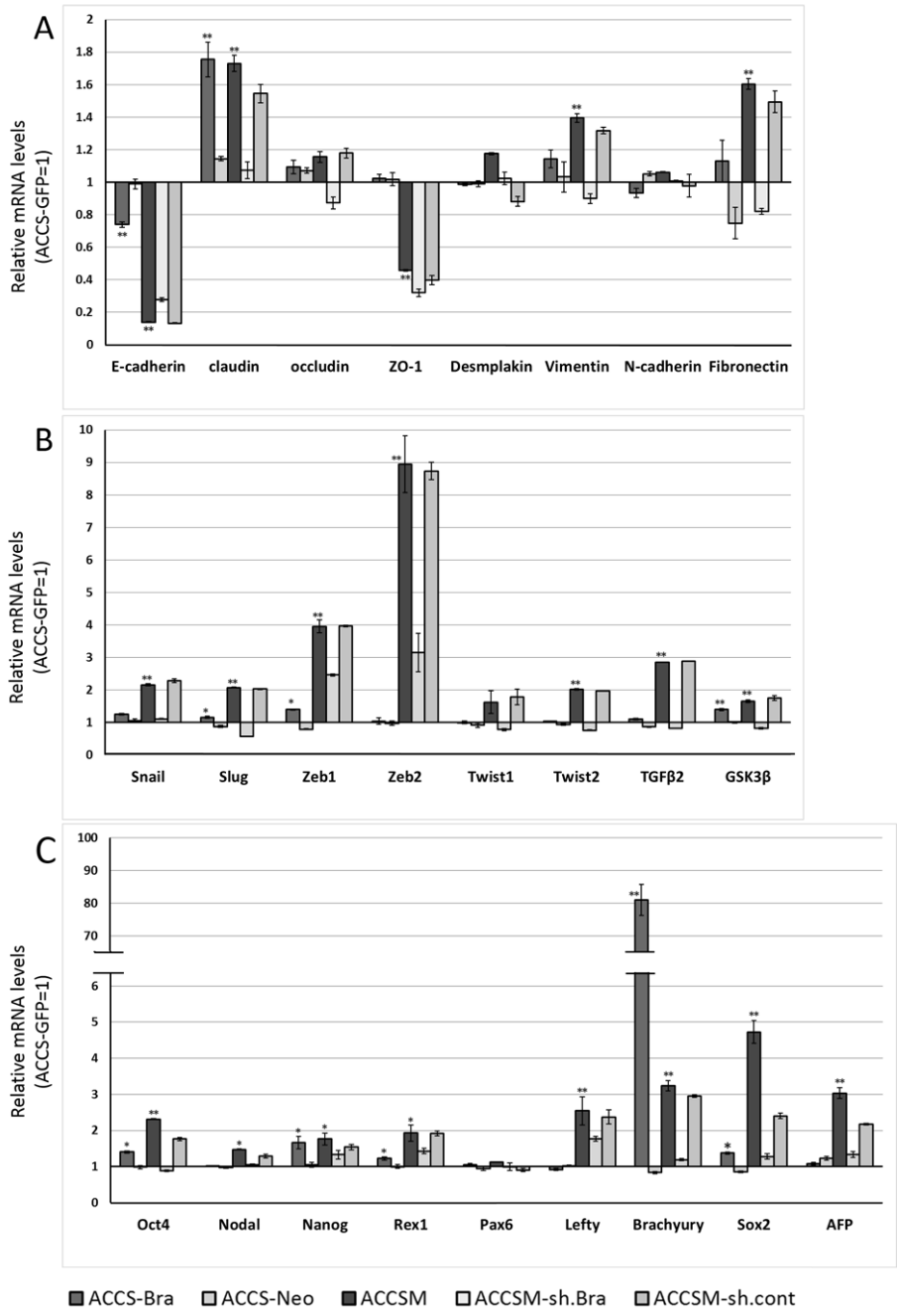

Figure 2. Effects of *BRACHYURY* transfection on gene expression related to epithelial–mesenchymal transition (EMT) and the cancer stem cell (CSC) phenotype in ACCS cells.

mRNA expression levels of the indicated genes in ACCS cells and in derivative clones were quantified using real-time RT-PCR as described in method section. Each mRNA level was compared with that in ACCS-GFP cells (parental cell line), and the data are shown in arbitrary units as relative mRNA levels (ACCS-GFP = 1.0). The expression levels of EMT-related genes (**A**, **B**), stem cell markers, and differentiation markers (**C**) are shown. The experiments were performed in triplicate, and the data were calculated as mean ± SD. Statistical significance of differences was analysed using the Student's t test. *$P < 0.05$, **$P < 0.01$.

3. Forced Co-Expression of BRACHYURY and SOX2 Induced the Self-Renewal Phenotype in Adenoid Cystic Carcinoma Cell Lines

SOX2, one of the stem cell transcription factor, is a critical regulator of tumor development and progression. The data from forced expression and a knockdown of Brachyury in oral carcinoma cell lines suggests that Brachyury may need a partner to drive the expression of the CSC phenotype. Therefore, we next analysed the effect of forced co-expression of *BRACHYURY* and *SOX2* on the self-renewal capacity. To this end, we established *SOX2* transfectants and *BRACHYURY* + *SOX2* co-expression transfectants of ACCS-GFP cells: ACCS-Sox2, and ACCS-Bra/Sox2. Forced expression of *SOX2* enhanced sphere formation (the number of spheres) in the primary sphere assay compared to parental cells ACCS-GFP (9.3-fold), but failed to increase the number of spheres in the secondary sphere assay. In contrast, co-expression of *BRACHYURY* and *SOX2* enhanced sphere formation in both the primary and the secondary sphere assays, with respect to both the diameter and the number of spheres, in ACCS cells. This enhancement reached the level of ACCS-M GFP cells (Figure 3). Forced expression of *SOX2* or co-expression of *BRACHYURY* and *SOX2* did not change the cell proliferation rate on cell culture dish (data not shown).

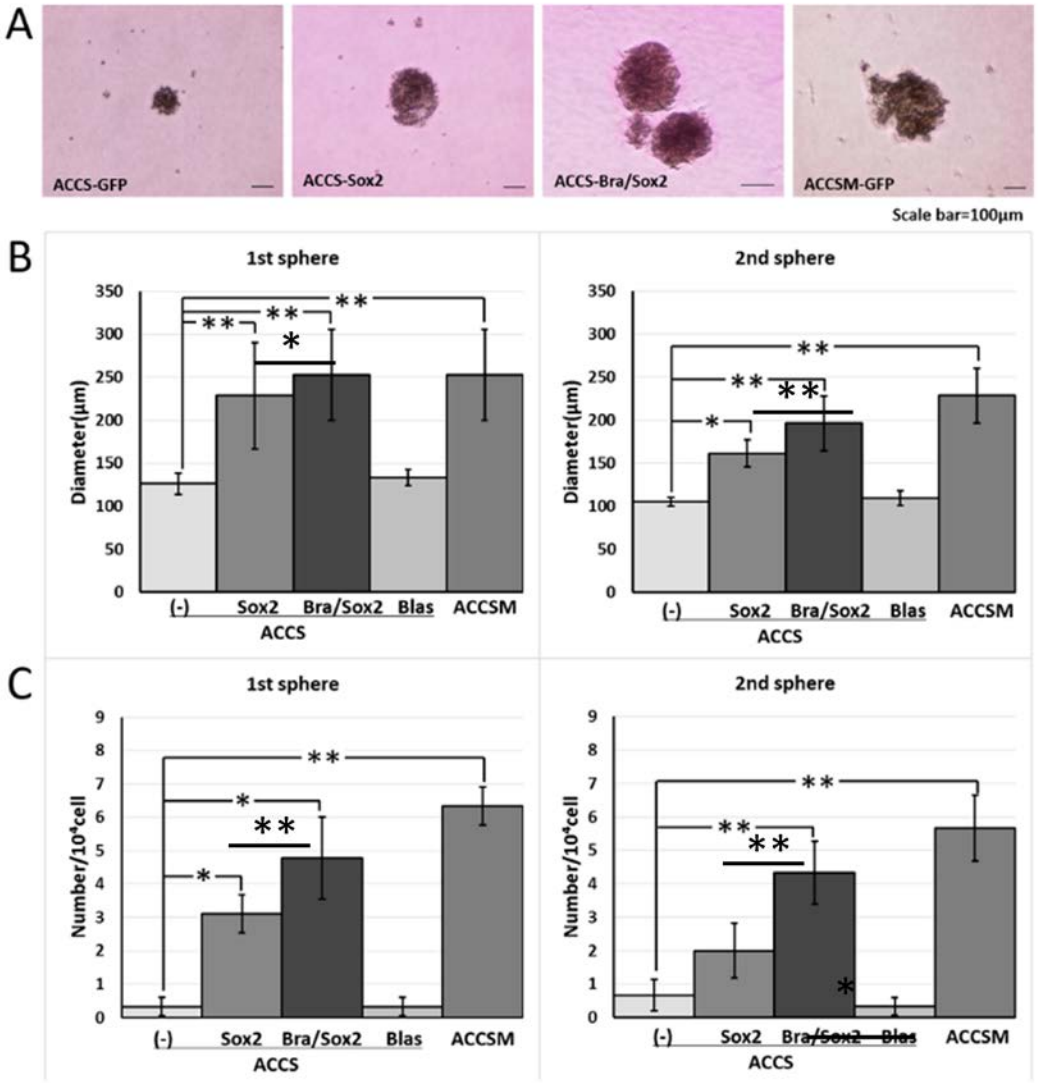

Figure 3. Effects of *BRACHYURY* and *SOX2* transfection on the sphere-forming ability of ACCS (adenoid cystic carcinoma) cells.

ACCS-Sox2, ACCS-Blasticidin (Blas) and ACCS-Bra/Sox2 cells were cultured, and the sphere-forming ability was quantified as described in the legend of Figure 1. Images of phase contrast microscope (**A**). Sphere diameters ($P < 0.0001$, ANOVA) (**B**), and Sphere numbers ($P < 0.0001$, ANOVA) (**C**) were analysed as described in the legend of Figure 1. The experiments were performed in triplicate, and the data were calculated as mean ± SD. Statistical significance of differences was analysed using the Student's t test. * $P < 0.05$, ** $P < 0.01$.

4. Forced Co-Expression of BRACHYURY and SOX2 Induced EMT-Related Markers and Stem Cell Markers in oral Cancer Cell Lines

We next analysed the effect of *SOX2* and co-expression of *BRACHYURY* and *SOX2* on EMT-related markers and stem cell markers in ACCS (Figure 4A-C) cell line in the same way as shown in Figure 3. The expression levels of EMT-related genes (Figure 4A), stem cell markers (Figure 4B), and differentiation markers (Figure 4C) are shown. In ACCS cells, forced expression of *SOX2* caused a significant increase in mRNA expression of *VIMENTIN, N-CADHERIN, FIBRONECTIN, SNAIL, SLUG, ZEB1, TGF-β2, GSK3β, OCT4, and NANOG* and caused a decrease in *E-CADHERIN* mRNA (Figure 4A-C). Co-expression of *BRACHYURY* and *SOX2* had synergistic effects on the enhancement of mRNA expression of *FIBRONECTIN*, *SNAIL*, *SLUG*, *ZEB1*, and *TGF-β2* in both cell lines. These synergistic effects on *FIBRONECTIN* and *TGF-β2* were especially strong.

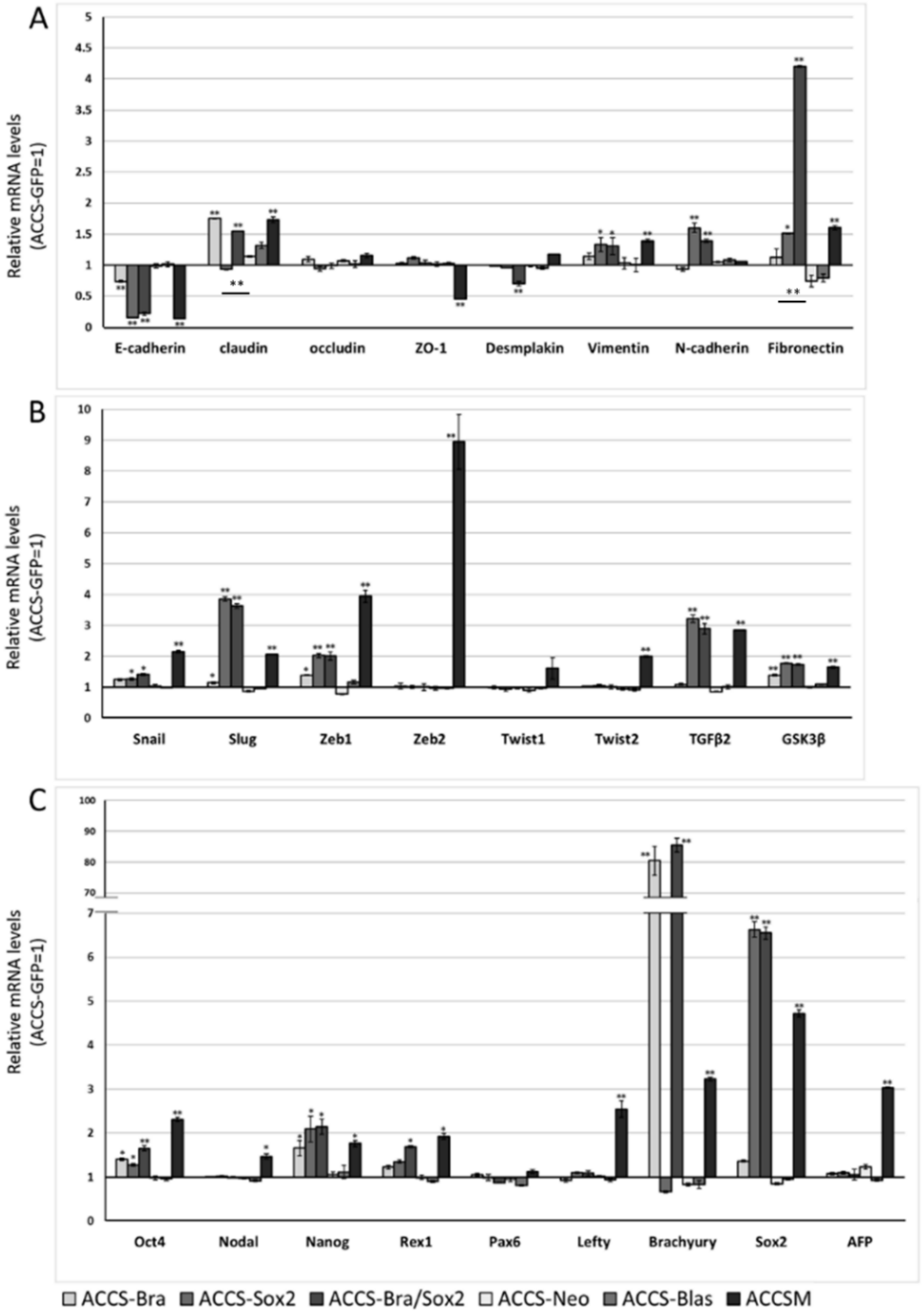

Figure 4. Effects of *BRACHYURY* and *SOX2* transfection on gene expression related to epithelial–mesenchymal transition (EMT) and cancer stem cell (CSC) phenotype in ACCS cells.

The mRNA expression levels of the indicated genes in ACCS (adenoid cystic carcinoma) cells and in derivative clones were quantified using real-time RT-PCR. Each mRNA level was compared with that in ACCS-GFP cells, and the data are shown in arbitrary units as relative mRNA levels (ACCS-GFP = 1.0). The expression levels of EMT-related genes (**A**, **B**), stem cell markers, and differentiation markers (**C**) are shown. The experiments were performed in triplicate, and the data were calculated as mean ± SD. Statistical significance of differences was analysed using the Student's t test. * $P < 0.05$, ** $P < 0.01$.

5. Artificial CSC-Like Cells Express An Invasive Phenotype In Vitro

The above results suggested that co-expression of *BRACHYURY* and *SOX2* induces the CSC phenotype. We then tested whether these artificial CSC-like cells show signs of invasiveness in vitro. The effect of forced expression of *BRACHYURY* or/and *SOX2* on cell migration of oral cancer cells in vitro was analysed using a wound healing assay (Figure 5). Cell migration of ACCS-M GFP cells was approximately 2 times faster than that of ACCS GFP cells. Expression of *BRACHYURY* or *SOX2* increase the cell migration ($P < 0.01$) but failed to reach the level of ACCS-M.

Co-expression of *BRACHYURY* and *SOX2* increased cell migration almost to the level of the CSC-like cells. There was no significance between ACCS-M GFP and ACCS Bra/Sox 2 ($P = 0.183$) (Figure 5A, B).

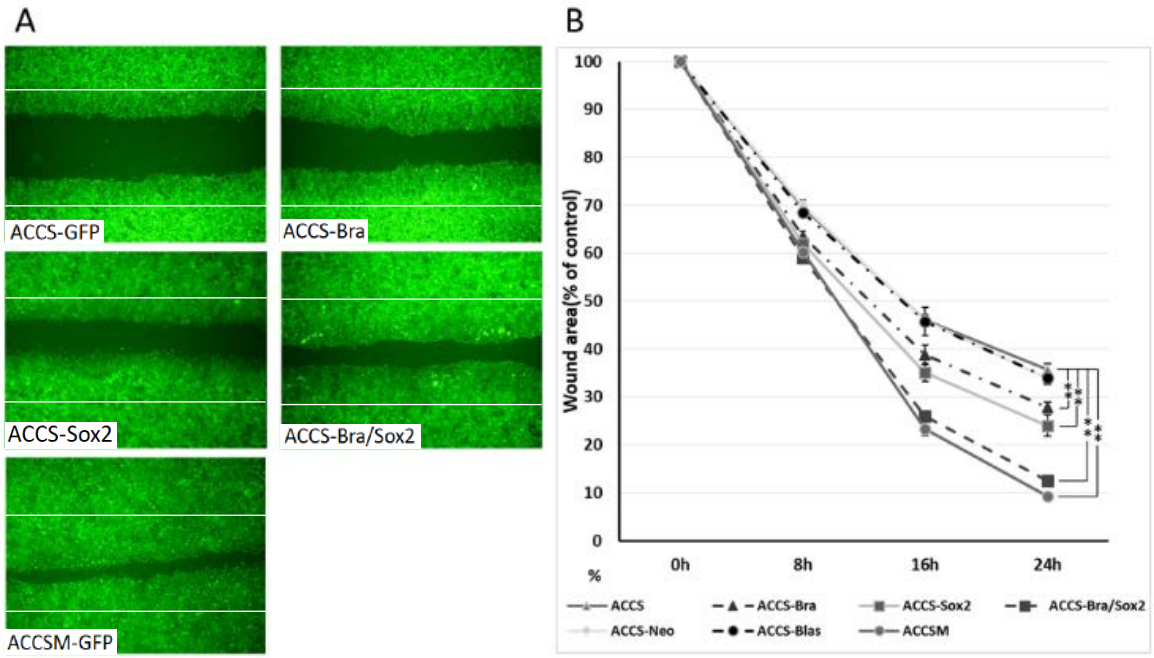

Figure 5. Effects of *BRACHYURY* and *SOX2* transfection on cell migration of ACCS cells.

(**A**) ACCS (adenoid cystic carcinoma) cells and derivative clones were seeded at 3×10^5 cells per well in a 6-well plate and incubated for 24 h so that a confluent monolayer of cells could form. After 24 h, scratch wounds were inflicted on the confluent monolayer of cells (white line) and incubation was continued for a further 24 h. Randomly chosen wound fields were photographed under a fluorescence microscope in the course of 24 h every 8 h. (**B**) The wound areas were evaluated using the following formula: wound area (% of control) = (wound area after the indicated period / initial wound area) × 100. The experiments were performed in triplicate, and the data were calculated as mean ± SD and ANOVA ($P < 0.0001$). Statistical significance of differences was analysed using the Student's t test. * $P < 0.05$, ** $P < 0.01$.

We next analysed the effect of forced expression of *BRACHYURY* or/and *SOX2* on cell invasiveness in vitro using a tumor cell dissemination assay that we established previously [22]. In this assay, carcinoma cells invade to artificial stroma (fibroblast embedded collagen gel) are visualised as fluorescent spots migrating from artificial primary cancer nest (cancer cell pellet solidified with collagen gel). Cancer cell invasiveness is evaluated by the number of invasive cells and their distance from the artificial primary cancer nest. As shown in Figure 6A, ACCS-M GFP cells invaded into artificial stroma very aggressive manner. Co-expression of *BRACHYURY* and *SOX2* strongly enhanced the invasiveness of ACCS-GFP cells to the level of the aggressive ACCS-M GFP cells *(P* = 0.223*)* (Figure 6A, B). Figure 6B shows the comparison of invasiveness among the ACCS cell lines. Relative invasiveness values (ACCS GFP = 1.0 arbitrary unit) were 3.7 (ACCS-Bra), 4.1 (ACCS-Sox2), 5.0 (ACCS-Bra/Sox2), and 5.6 (ACCS-M GFP). Expression of *BRACHYURY* or *SOX2* increase the cell invasiveness ($P < 0.01$) but failed to reach the level of ACCS-M.

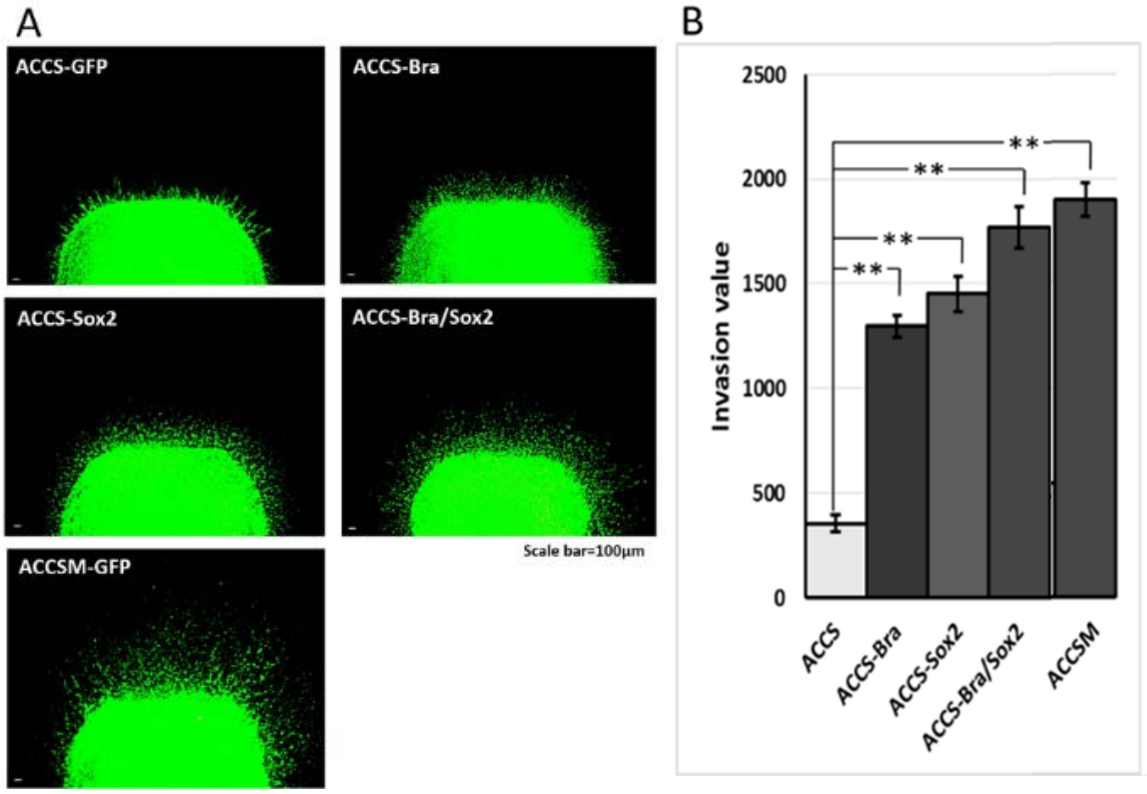

Figure 6. Effects of *BRACHYURY* and *SOX2* transfection on cell invasiveness of ACCS cells. One million ACCS cells each were pelleted and solidified as described in Materials and Methods.

The collagen-embedded tumor cells were embedded in the collagen-embedded fibroblasts and allowed to invade into artificial stroma. After 7 days, tumor dissemination was observed under a fluorescence microscope (**A**). Tumor dissemination from the tumor cell pellet was evaluated in 5 randomly selected standardised rectangular light fields (500 × 100 μm), and the values were summed as described in Materials and Methods (**B**). The experiments were performed in triplicate, and the data were calculated as mean ± SD and ANOVA ($P < 0.0001$). Statistical significance of differences was analysed using the Student's t test. * $P < 0.05$, ** $P < 0.01$.

6. BRACHYURY and SOX2 shRNA do not influence growth of ACCS cell lines.

We established ACCS GFP and ACCS-M GFP-derived cell lines by stable transfection of *BRACHYURY* or *SOX2* shRNA lentiviral plasmids. The expression level of *BRACHYURY* or *SOX2* in shRNA-transfected ACCS cells was monitored by real-time RT-PCR to confirm silencing of the target genes (Fig. 7A). We first analyzed the effect of *BRACHYURY* or *SOX2* knockdown on cell growth *in vitro* by MTT assay. Cancer stem cell-like ACCS-M GFP cells demonstrated a similar growth pattern to parental ACCS GFP cells. Stable transfection of shRNA did not affect cell growth (ACCS-M sh cont. GFP). Neither *BRACHYURY* shRNA nor *SOX2* shRNA affected cell growth (ACCS-M shBr GFP and ACCS-M sh*SOX2* GFP, respectively; Fig. 7B).

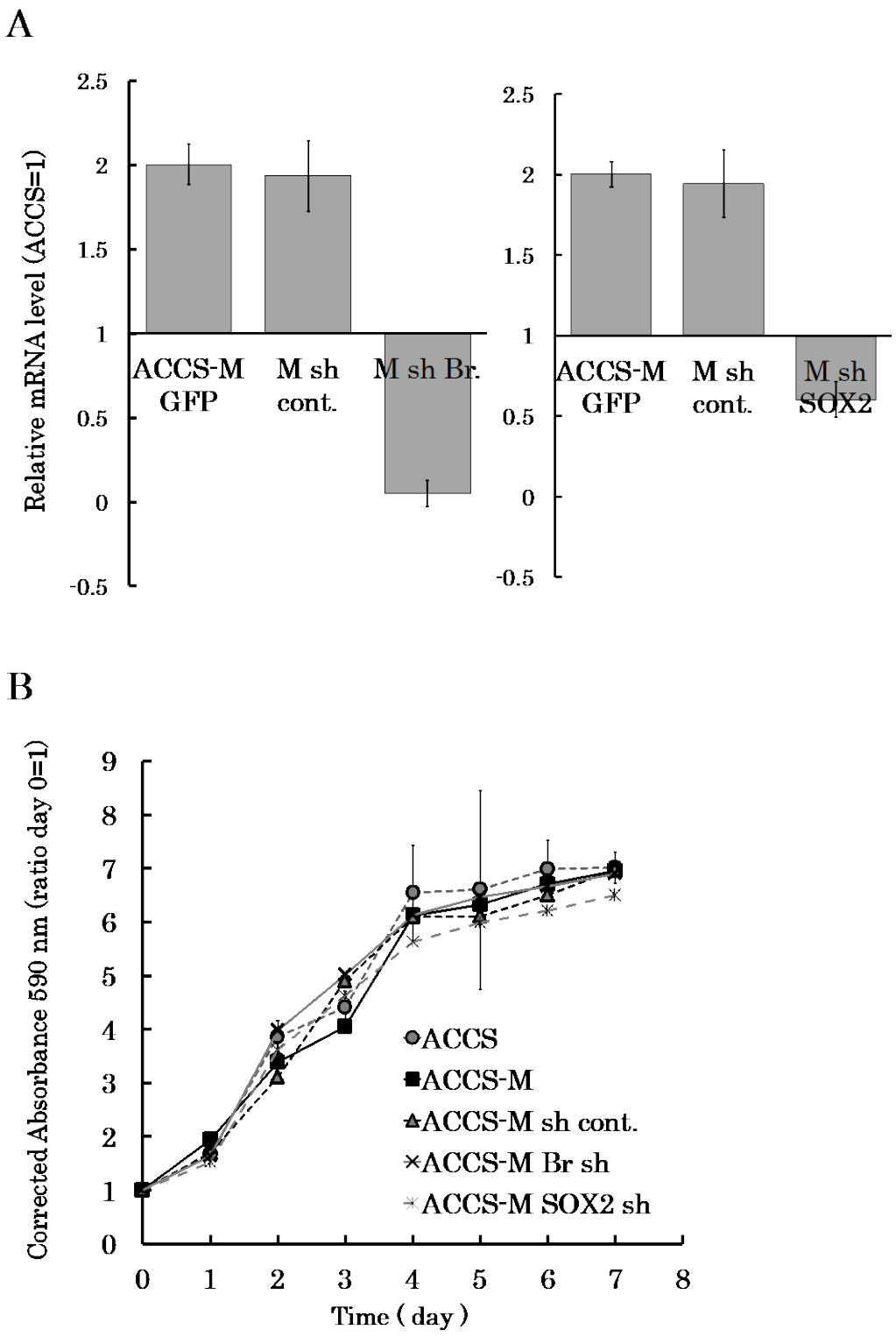

Figure 7: Effect of *BRACHYURY* and *SOX2* knockdown on ACCS cell growth.

(A) The mRNA expression levels of *BRACHYURY* and *Sox2* in shRNA-transfected cells as quantified by real-time RT-PCR. Data are shown as mRNA levels relative to ACCS GFP. Error bars indicate the standard deviation.
(B) Cell growth of ACCS and its derivatives, as evaluated by MTT assay. Error bars indicate the standard deviation.

7. BRACHYURY shRNA inhibits cell migration

The effect of *BRACHYURY* or *SOX2* knockdown on cell migration *in vitro* was analyzed by the wound healing assay (Fig. 8). Cell migration of ACCS-M GFP cells was approximately twice as fast as that of ACCS GFP cells. *BRACHYURY* knockdown significantly inhibited migration of ACCS-M GFP cells to the level of parental ACCS GFP ($P = 0.001$). By contrast, *SOX2* knockdown had no effect on ACCS-M GFP cell migration.

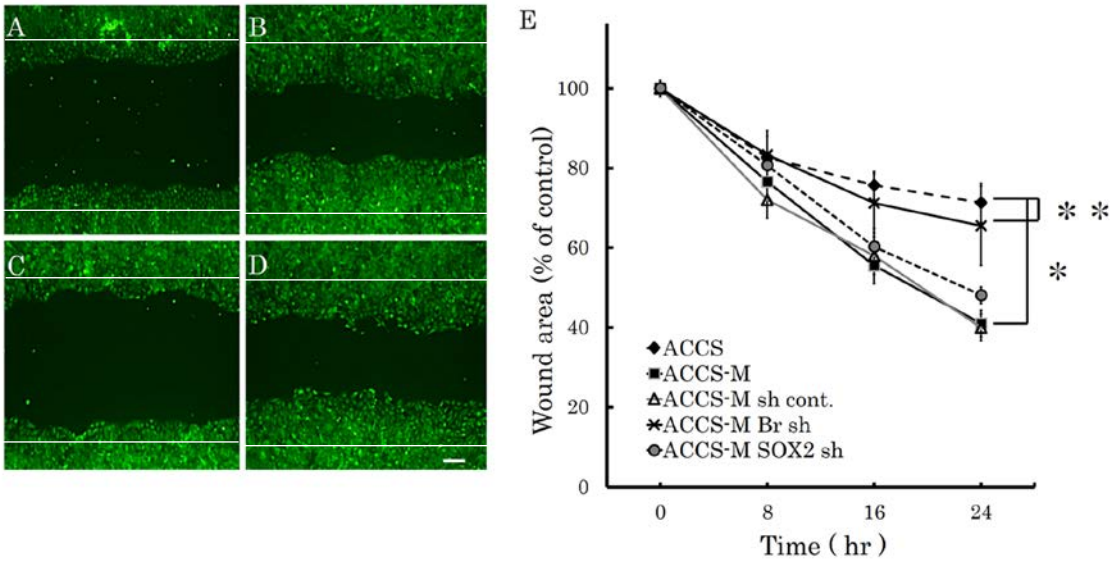

Figure 8. Effect of *BRACHYURY* and *SOX2* knockdown on ACCS cell migration.
Cell migration, as evaluated by the wound-healing assay. Photomicrographs of wound regions 24 h after the start of the assay (A–D). (A) ACCS GFP, (B) ACCS-M GFP, (C) ACCS-M shBr GFP, and (D) ACCS-M shSOX2 GFP cells. Bar = 100 μm. (E) Calculated wound area. *$P < 0.001$, **$P < 0.05$.

8. BRACHYURY and SOX2 shRNA inhibit cell invasion

We next analyzed the effect of *BRACHYURY* or *SOX2* knockdown on cell invasiveness *in vitro* using tumor-cell dissemination assay (25). As shown in Figure 9B, ACCS-M GFP cells demonstrated aggressive cell invasion into artificial stromal tissue. Invasiveness of ACCS-M GFP cells was strongly inhibited by knockdown of *BRACHYURY* (Fig. 9C) or *SOX2* (Fig. 9D). Figure 3E compares invasiveness among ACCS cell lines. Relative invasiveness values (ACCS GFP = 1) were 6.4 (ACCS-M GFP), 2.3 (ACCS-M shBr GFP), and 3.2 (ACCS-M shSOX2 GFP).

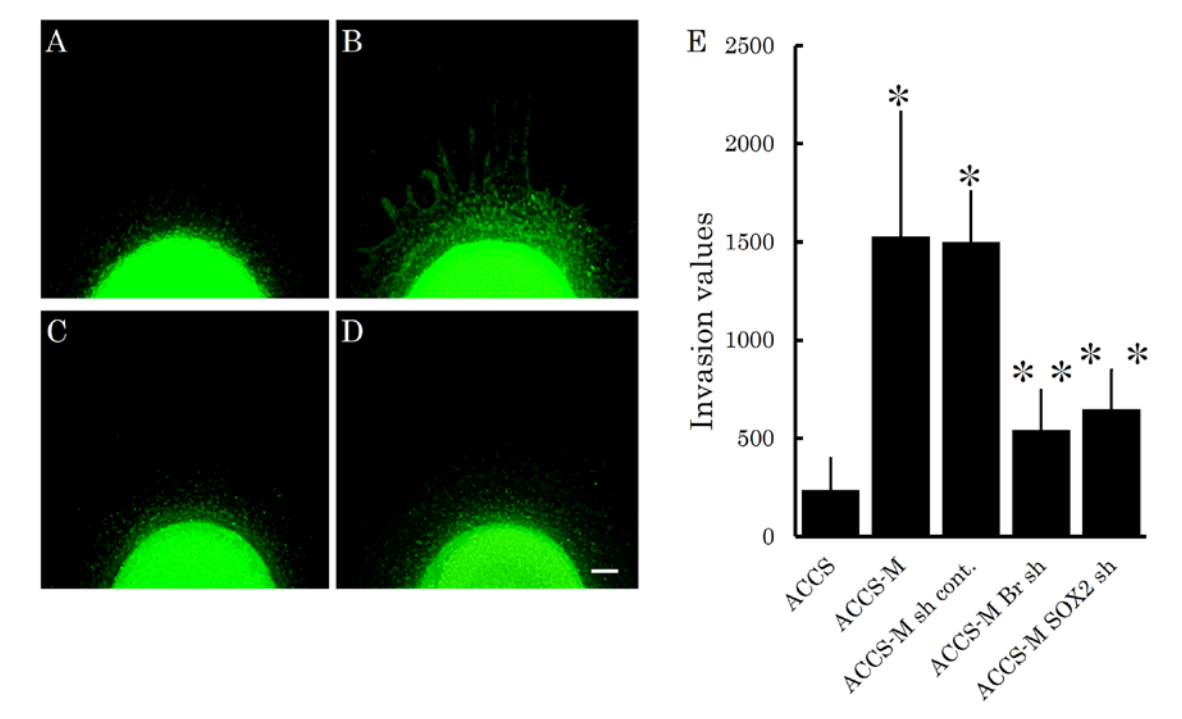

Figure 9: Effect of *BRACHYURY* and *SOX2* knockdown on ACCS cell invasiveness. ACCS GFP (A), ACCS-M GFP (B), ACCS-M shBr GFP(C), and ACCS-M shSOX2 GFP cells (D) as analyzed with the new invasion assay. Photomicrographs taken after a 7-day incubation. Bar = 100 µm. (E) Error bars indicate standard deviation. **P* < 0.001, ***P* < 0.05.

9. Knockdown of the BRACHYURY inhibits tumorigenicity and metastasis in vivo

The effect of *BRACHYURY* knockdown on ACCS-M GFP tumorigenicity and metastasis *in vivo* was examined using a mouse metastasis model established and reported by Ishii *et al.*[3]. Figure 10A shows a typical tumor in tongue (a–c), its GFP excitation (d–f), and submandibular lymph node metastasis (g–i). Remarkably, ACCS-M shBra sometimes failed to develop into tongue tumor (50% tumorigenicity), and metastasis was completely inhibited. ACCS-M sh*SOX2* also reduced tumorigenicity (87.5%) and metastasis (87.5%), but the impact of inhibition was more relevant with ACCS-M shBra (Table 2). Tumor growth rate was also significantly inhibited in ACCS-M shBra cells (Figure 10B).

Table 2. Tumorigenicity and metastasis of each cell line

	Tumorigenicity		Metastasis	
Cell line	Tumorigenic mouse (%)	Tumor volume (mm3)	*SMLN (%)	LUNG (%)
ACCS-M GFP	8/8 (100)	145.3	8/8 (100)	7/8 (87.5)
ACCS-M sh cont.	8/8 (100)	121.4	8/8 (100)	7/8 (87.5)
ACCS-M sh Br.	4/8 (50)	28.3	N.D	N.D
ACCS-M sh SOX2	7/8 (87.5)	37.2	7/8 (87.5)	3/8 (37.5)

*Submandibular lymph nodes. N.D: not detected

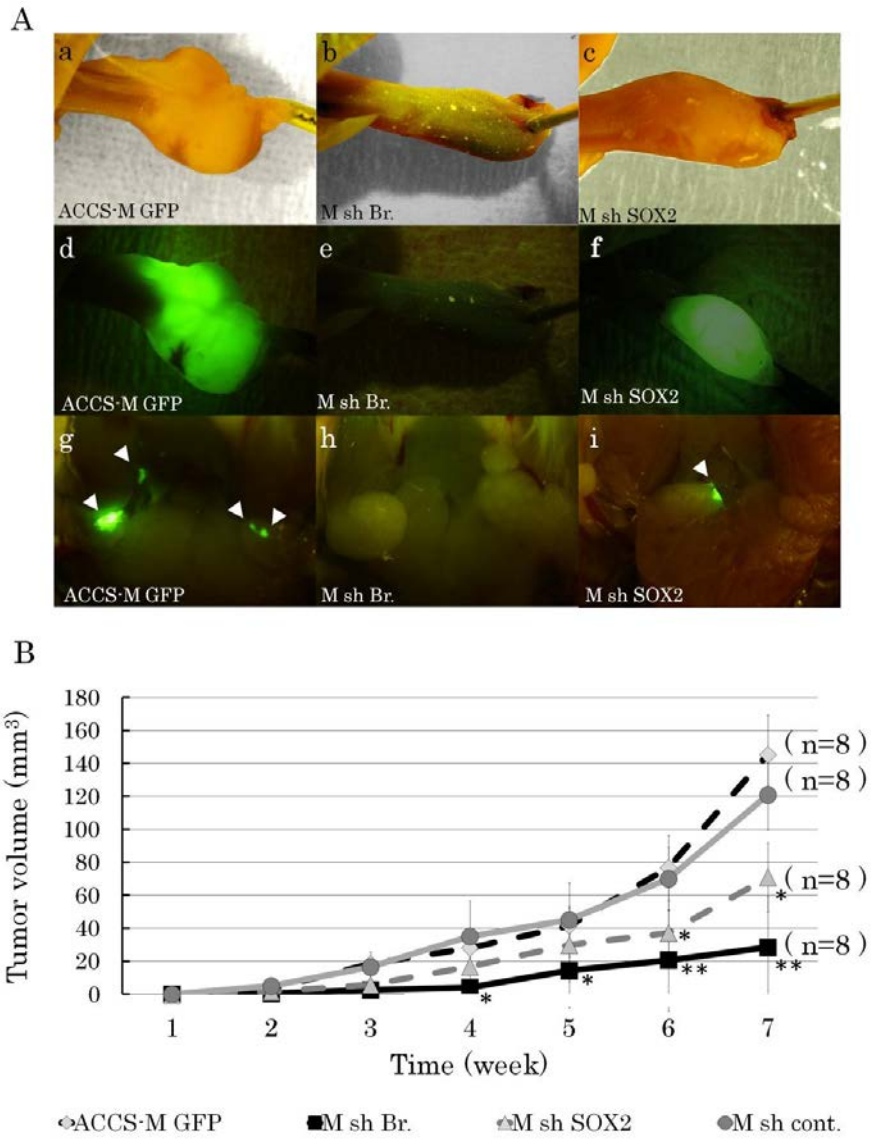

Figure 10: *BRACHYURY* silencing reduces the tumorigenicity and metastasis of ACCS-M GFP cells.

A. ACCS-M GFP derivatives transfected with shRNAs (untreated control, ACCS-M GFP [**a**, **d**, **g**]; *BRACHYURY* shRNA, M sh.Bra [**b**, **e**, **h**]; *SOX2* shRNA, M sh. *SOX2* [**c**, **f**, **i**]) were injected into the tongues of nude mice and examined to detect tumors in tongues (a–f) and spontaneous metastases in submandibular lymph nodes (**g**–**i**). Observations with the naked eye (**a**–**c**) and the excitation of GFP (**d**–**i**) are shown. Sites of lymph node metastasis are labeled with arrowheads. Note that GFP enables the detection of micro-metastasis in the lymph nodes. **B**. The primary tumor volumes were measured weekly, calculated as the length × width × thickness, and mice were sacrificed when the primary tumor volume reached 100 mm^3. Tumor growth curves for ACCS derivatives ACCS-M GFP (diamond), sh.Bra (square), sh. *SOX2* (triangle), and sh cont. (control shRNA, circle) are shown. Experiments were performed in 6 mice for each ACCS derivative, and the values were averaged. Bars indicate the standard deviation. Data significances between ACCS-M GFP and other ACCS derivatives were analyzed by Student's *t*-test. $*P < 0.05$, $**P < 0.01$.

Discussion

Metastasis is a most life-threatening event which directly influencing prognosis in cancer progression. Accumulated evidences suggest that cancer invasion and metastasis is strongly regulated by EMT in cancer cells [23–25]. Similarly, CSCs have attracted more and more attention as targets for cancer therapy because they have been reported to exhibit chemo- and radio-resistance [15,16,26–28]. More recently, the direct link between EMT and CSC phenotype was reported [6,23,29,30], but the regulatory mechanisms behind cancer stemness and EMT are still unclear.

In this study, we showed that CSC phenotypes, including EMT, and tumorigenic/metastatic potential could be blocked by knocking down the transcriptional factor *BRACHYURY* in vitro and in vivo. This finding suggests that *BRACHYURY* is a key regulator of the CSC phenotype. Sarkar et al. [31] also reported that a *BRACHYURY* knockdown via siRNA resulted in downregulation of expression of *CD44*, *CD166*, *CD133*, *ALDH1*, and *NANOG* in colon cancer, and they concluded that *BRACHYURY* participates in establishment of CSC characteristics by inducing *NANOG* expression. In the present study, we showed that overexpression of *BRACHYURY* upregulated *NANOG* expression slightly, but failed to promote self-renewal capacity in ACCS GFP (adenoid cystic carcinoma) cells. Fernando et al. [20] reported that forced expression of *BRACHYURY* caused induction of EMT (gain of mesenchymal markers and loss of epithelial markers) and increased in cell migration and invasion in human carcinoma cell line. In this regard, our results completely match their findings. It is thought that *NANOG* is not absolutely required for self-renewal of embryonic stem cells but is required for pluripotency [32]. In line with this notion, in our present experiments, *BRACHYURY* overexpression promoted only the EMT phenotype, a type of invasive phenotype. Some authors proposed to classify EMT into 3 subtypes based on

biological status with biomarkers [33,34]. Type 1; EMT associated with organ development, Type 2; EMT related to wound healing and regeneration. EMT in cancer progression and metastasis is categorized as type 3 EMT and specific signaling or biomarkers has yet to be determined. *TGF-β* would be the most responsible factor for induction of EMT by inducing EMT-inducing transcription factors in cancer cells, notably *SNAIL, SLUG, ZEB1, TWIST, GOOSECOID,* and *FOXC2* [35].

SOX2 (SRY Sex Determining Region Y-Box2) is a member of the Sox (SRY-related HMG box) family of transcription factors. *SOX2* maintains stemness and pluripotency of normal stem cells by regulating gene transcription. Recent reports revealed the association between *SOX2* and EMT [36,37]. In line with these reports, *SOX2* overexpression resulted in specific changes in EMT of ACCS-Sox2 cells in the present work. It is also well known that *SOX2* promotes metastasis of breast and prostate cancer cells via activation of the Wnt/β-catenin pathway [38]. *SOX2* protein binds to the promoter region of β-catenin and regulates its expression. In addition, *SOX2* protein regulates the protein expression of downstream elements in Wnt signaling, DKK3, DVL1, and DVL3 [38]. Aberrant activation of Wnt/β-catenin signaling has been described in a variety of cancers, and inhibition of Wnt/β-catenin by DKK-1 resulted in diminution of the self-renewal capacity of a gastric cancer cell line [39]. Overexpression of *SOX2* increased the self-renewal capacity in ACCS GFP cells in the present work. Nonetheless, the self-renewal capacity of ACCS-Sox2 cells was approximately 50% in size and 30% in number compared to ACCS-M GFP cells, even though *SOX2* expression was 150% higher in ACCS-Sox2 cells. These data suggest that *SOX2* promotes EMT and self-renewal capacity, but it is not a key player in these processes.

Several factors have been reported as indispensable for stem cell maintenance and differentiation. For example, *OCT3/4, SOX2, KLF-4, and C-MYC* are necessary for expression of the phenotype of induced pluripotent stem cells in human and mouse fibroblasts [40, 41]. These factors have been reported to physically or synergistically interact

with each other during development [42]. The same kind of protein or gene network may exist in cancer stem cells. Chen et al. reported that silencing of the *SOX2* gene reduces the tumorigenic potential of a lung cancer cell line (A549 cells) with downregulation of *C-MYC, WNT1, WNT2, and NOTCH1* in mice; these authors uncovered 246 additional target cancer genes of *SOX2* [43]. In the present work, we found significant upregulation of *TGF-β* and fibronectin as a result of simultaneous overexpression of *SOX2* and *BRACHYURY*. This synergistic effect of *SOX2* and *BRACHYURY* in the promotion of the invasive phenotype of CSCs, especially when it comes to *TGF-β* and *FIBRONECTIN* expression, could be explained by the same kind of protein or signaling network as mentioned above.

SOX2 activates the Wnt/β-catenin pathway and causes β-catenin activation [38], and the target gene of this activated β-catenin is *BRACHYURY* [44]. It was shown that *BRACHYURY* promotes the EMT phenotype and positively relate each other with *TGF-β* in mesenchymal-like tumor cells [45,46]. *BRACHYURY* stimulates *TGF-β1* expression, and overexpressed *TGF-β1* induces *SOX2* in turn [47]. *SOX2* also positively regulates *FIBRONECTIN* expression [48], and *FIBRONECTIN* enhances the EMT phenotype and self-renewal capacity [49]. Therefore, a potentially unlimited autocrine loop is expected to be established among *SOX2*, *BRACHYURY*, *TGF-β*, and *FIBRONECTIN*. As discussed above, *BRACHYURY* mainly plays a role in EMT, and *SOX2* is involved in EMT and self-renewal. Their synergistic effect, however, may be more crucial because the interaction of the *SOX2* and *BRACHYURY* gene networks activates a vast network of genes/proteins that drives the development of cancer invasiveness. In other words, the closer to the centre of the network (*SOX2* and *BRACHYURY*) a target factor is, the greater the impact of its inactivation on EMT and cancer stemness. This is why silencing of *BRACHYURY* is observed to be so effective.

In this study, we showed that co-expression of *BRACHYURY* and *SOX2* promotes both EMT and self-renewal phenotypes in ACCS-GFP cells; phenotypes that resemble ACCS-M GFP, the CSC-like cell line from in vivo selection. Nonetheless, the patterns of the

expression of some genes (e.g., *ZEB2*) are still different between ACCS-M GFP cells and ACCS Bra/Sox2. We could not enhance *ZEB2* expression by co-expressing *BRACHYURY* and *SOX2*. The role of *ZEB2* in CSCs is not clear, and further research is needed to identify which factor(s) control *ZEB2* expression and its function in cancer stemness.

As mentioned above, *BRACHYURY* and *SOX2* were not sufficient for initiation of cancer stem cell property, especially pluripotency related genes. However, it is also true that *BRACHYURY* is required for tumorigenesis and metastasis, the most important property for cancer stem cell in vivo. We showed that *BRACHYURY* knockdown completely inhibits CSC and EMT phenotypes of the ACCS-M GFP cells. These findings support a crucial role of *BRACHYURY* in the regulation of cancer stemness in adenoid cystic carcinoma cell lines. It was also confirmed that protein expression of Brachyury strongly correlates with EMT and metastasis involvement in oral cancer patients [5].

These results will provide important clues as to how the CSC phenotype is developed via accumulating alterations in gene networks and why this phenomenon is very similar to developmental processes with respect to their effects, but is completely different with respect to their mechanisms. When all pieces of the puzzle are in place, researchers will be able to explain why cells expressing the EMT phenotype sometimes fail to metastasise [50–52] and why cancer stemness exhibits heterogeneity.

Conclusion

We conclude that *BRACHYURY* and *SOX2* synergistically promote EMT (invasiveness) and self-renewal property, and one of the members of cancer stemness related genes. This new knowledge is expected to lead to more specific and effective therapeutic targets in oral cancer, which may include *SOX2* and *BRACHYURY*, either alone or in combination.

Acknowledgments:

稿を終えるにあたり、本研究の課題を与え、実験方法や指針など真摯にご指導頂き、御校閲頂きました、杉浦 剛 教授に深謝致します。また、本研究を遂行するにあたり、実験手技等の御指導、御助言頂きました　浜田　倫史　講師、九州大学大学院　歯学研究院　口腔顎顔面病態学講座　口腔顎顔面外科学分野　秋本　直柔　博士に深く感謝致します。また、様々な御助言や励ましのお言葉を頂いた、鹿児島大学大学院　医歯学総合研究科　顎顔面機能再建学講座　顎顔面制御学分野の皆様、研究生活を支えてくださった全ての皆様に心より感謝致します。

References

1. Chang, C.C.; Hsu, W.H.; Wang, C.C.; Chou, C.H.; Kuo, M.Y.; Lin, B.R.; Chen, S.T.; Tai, S.K.; Kuo, M.L.; Yang, M.H. **Connective tissue growth factor activates pluripotency genes and mesenchymal-epithelial transition in head and neck cancer cells.** *Cancer Res.* 2013, *73*, 4147–4157.

2. Drasin, D.J.; Robin, T.P.; Ford, H.L. **Breast cancer epithelial-to-mesenchymal transition: Examining the functional consequences of plasticity.** *Breast Cancer Res.* 2011, *13*, 226.

3. Pirozzi, G.; Tirino, V.; Camerlingo, R.; La Rocca, A.; Martucci, N.; Scognamiglio, G.; Franco, R.; Cantile, M.; Normanno, N.; Rocco, G. **Prognostic value of cancer stem cells, epithelial-mesenchymal transition and circulating tumor cells in lung cancer.** *Oncol. Rep.* 2013, *29*, 1763–1768.

4. Zubeldia, I.G.; Bleau, A.M.; Redrado, M.; Serrano, D.; Agliano, A.; Gil-Puig, C.; Vidal-Vanaclocha, F.; Lecanda, J.; Calvo, A. **Epithelial to mesenchymal transition and cancer stem cell phenotypes leading to liver metastasis are abrogated by the novel TGFbeta1-targeting peptides P17 and P144.** *Exp. Cell Res*. 2013, *319*, 12–22.

5. Imajyo, I.; Sugiura, T.; Kobayashi, Y.; Shimoda, M.; Ishii, K.; Akimoto, N.; Yoshihama, N.; Kobayashi, I.; Mori, Y. **T-box transcription factor Brachyury expression is correlated with epithelial-mesenchymal transition and lymph node metastasis in oral squamous cell carcinoma.** *Int. J. Oncol*. 2012, *41*, 1985–1995.

6. Mani, S.A.; Guo, W.; Liao, M.J.; Eaton, E.N.; Ayyanan, A.; Zhou, A.Y.; Brooks, M.; Reinhard, F.; Zhang, C.C.; Shipitsin, M.; et al. **The epithelial-mesenchymal transition generates cells with properties of stem cells.** *Cell* 2008, *133*, 704–715.

7. Hindriksen, S.; Bijlsma, M.F. **Cancer stem cells, EMT, and developmental pathway activation in pancreatic tumors.** *Cancers* 2012, *4*, 989–1035.

8. Zhang, S.S.; Han, Z.P.; Jing, Y.Y.; Tao, S.F.; Li, T.J.; Wang, H.; Wang, Y.; Li, R.; Yang, Y.; Zhao, X.; et al. **CD133(+)CXCR4(+) colon cancer cells exhibit metastatic potential and predict poor prognosis of patients.** BMC *Med.* 2012, *10*, 85.

9. Mallini, P.; Lennard, T.; Kirby, J.; Meeson, A. **Epithelial-to-mesenchymal transition: What is the impact on breast cancer stem cells and drug resistance.** *Cancer Treat. Rev.* 2014, *40*, 341–348.

10. Wood, S.L.; Pernemalm, M.; Crosbie, P.A.; Whetton, A.D. **The role of the tumor-microenvironment in lung cancer-metastasis and its relationship to potential therapeutic targets.** *Cancer Treat. Rev.* 2014, *40*, 558–566.

11. Gupta, P.B.; Chaffer, C.L.; Weinberg, R.A. **Cancer stem cells: Mirage or reality?** *Nat. Med*. 2009, *15*, 1010–1012.

12. Brabletz, S.; Brabletz, T. **The ZEB/miR-200 feedback loop--a motor of cellular plasticity in development and cancer?** *EMBO Rep.* 2010, *11*, 670–677.

13. Fuxe, J.; Vincent, T.; Garcia de Herreros, A. **Transcriptional crosstalk between TGFβ**

and stem cell pathways in tumor cell invasion: Role of EMT promoting Smad complexes. *Cell Cycle* 2010, *9*, 2363–2374.

14. Zheng, H.; Kang, Y. **Multilayer control of the EMT master regulators.** *Oncogene* 2014, *33*, 1755.

15. Wang, Z.; Li, Y.; Ahmad, A.; Banerjee, S.; Azmi, A.S.; Kong, D.; Sarkar, F.H. **Pancreatic cancer: Understanding and overcoming chemoresistance.** *Nat. Rev. Gastroenterol. Hepatol*. 2011, *8*, 27–33.

16. Singh, A.; Settleman, J. **EMT, cancer stem cells and drug resistance: An emerging axis of evil in the war on cancer.** ***Oncogene*** 2010, *29*, 4741–4751,.

17. Shekhani, M.T.; Jayanthy, A.S.; Maddodi, N.; Setaluri, V. **Cancer stem cells and tumor transdifferentiation: Implications for novel therapeutic strategies.** *Am. J. stem cells* 2013, *2*, 52–61.

18. Smalley, M.; Piggott, L.; Clarkson, R. **Breast cancer stem cells: Obstacles to therapy.** *Cancer Lett.* 2013, *338*, 57–62.

19. Palena, C.; Polev, D.E.; Tsang, K.Y.; Fernando, R.I.; Litzinger, M.; Krukovskaya, L.L.; Baranova, A.V.; Kozlov, A.P.; Schlom, J. **The human T-box mesodermal transcription factor Brachyury is a candidate target for T-cell-mediated cancer immunotherapy.** *Clin. Cancer Res*. 2007, *13*, 2471–2478.

20. Fernando, R.I.; Litzinger, M.; Trono, P.; Hamilton, D.H.; Schlom, J.; Palena, C. **The T-box transcription factor Brachyury promotes epithelial-mesenchymal transition in human tumor cells.** *J. Clin. Invest*. 2010, *120*, 533–544.

21. Ishii, K.; Shimoda, M.; Sugiura, T.; Seki, K.; Takahashi, M.; Abe, M.; Matsuki, R.; Inoue, Y.; Shirasuna, K. **Involvement of epithelial-mesenchymal transition in adenoid cystic carcinoma metastasis.** *Int. J. Oncol.* 2011, *38*, 921–931.

22. Abe, M.; Sugiura, T.; Takahashi, M.; Ishii, K.; Shimoda, M.; Shirasuna, K. **A novel function of CD82/KAI-1 on E-cadherin-mediated homophilic cellular adhesion of cancer cells.** *Cancer Lett.* 2008, *266*, 163–170.

23. Biddle, A.; Mackenzie, I.C. **Cancer stem cells and EMT in carcinoma.** *Cancer Metastasis Rev.* 2012, *31*, 285–293.

24. Rhim, A.D.; Mirek, E.T.; Aiello, N.M.; Maitra, A.; Bailey, J.M.; McAllister, F.; Reichert, M.; Beatty, G.L.; Rustgi, A.K.; Vonderheide, R.H.; et al. **EMT and dissemination precede pancreatic tumor formation.** *Cell* 2012, *148*, 349–361.

25. Wellner, U.; Schubert, J.; Burk, U.C.; Schmalhofer, O.; Zhu, F.; Sonntag, A.; Waldvogel, B.; Vannier, C.; Darling, D.; zur Hausen, A.; et al. **The EMT-activator ZEB1 promotes tumorigenicity by repressing stemness-inhibiting microRNAs.** *Nature cell biol.* 2009, *11*, 1487–1495.

26. Nicolini, A.; Ferrari, P.; Fini, M.; Borsari, V.; Fallahi, P.; Antonelli, A.; Berti, P.; Carpi, A.; Miccoli, P. **Stem cells: Their role in breast cancer development and resistance to treatment.** *Curr. Pharm. Biotechno*. 2011, *12*, 196–205.

27. Yu, Z.; Pestell, T.G.; Lisanti, M.P.; Pestell, R.G. **Cancer stem cells.** *Int. J. Biochem. Cell Biol.* 2012, *44*, 2144–2151.

28. Morrison, C.D.; Parvani, J.G.; Schiemann, W.P. **The relevance of the TGF-beta**

Paradox to EMT-MET programs. *Cancer Lett.* 2013, *341*, 30–40.

29. Brabletz, T. **EMT and MET in metastasis: Where are the cancer stem cells?** *Cancer cell* 2012, *22*, 699–701.

30. Kong, D.; Banerjee, S.; Ahmad, A.; Li, Y.; Wang, Z.; Sethi, S.; Sarkar, F.H. **Epithelial to mesenchymal transition is mechanistically linked with stem cell signatures in prostate cancer cells.** *PLoS ONE* 2010, *5*, e12445.

31. Sarkar, D.; Shields, B.; Davies, M.L.; Muller, J.; Wakeman, J.A. **BRACHYURY confers cancer stem cell characteristics on colorectal cancer cells.** *Int. J. Cancer* 2012, *130*, 328–337.

32. Chambers, I.; Silva, J.; Colby, D.; Nichols, J.; Nijmeijer, B.; Robertson, M.; Vrana, J.; Jones, K.; Grotewold, L.; Smith, A. Nanog **Safeguards pluripotency and mediates germline development.** *Nature* 2007, *450*, 1230–1234.

33. Kalluri, R. EMT: **When epithelial cells decide to become mesenchymal-like cells.** *J. Clin. Invest.* 2009, *119*, 1417–1419.

34. Zeisberg, M.; Neilson, E.G. **Biomarkers for epithelial-mesenchymal transitions.** *J. Clin. Invest.* 2009, *119*, 1429–1437.

35. Heldin, C.H.; Vanlandewijck, M.; Moustakas, A. **Regulation of EMT by TGFβ in cancer.** *FEBS Lett*. 2012, *586*, 1959–1970.

36. Herreros-Villanueva, M.; Zhang, J.S.; Koenig, A.; Abel, E.V.; Smyrk, T.C.; Bamlet, W.R.; de Narvajas, A.A.; Gomez, T.S.; Simeone, D.M.; Bujanda, L.; et al. **SOX2 promotes dedifferentiation and imparts stem cell-like features to pancreatic cancer cells.** *Oncogenesis* 2013, *2*, e61.

37. Han, X.; Fang, X.; Lou, X.; Hua, D.; Ding, W.; Foltz, G.; Hood, L.; Yuan, Y.; Lin, B. **Silencing SOX2 induced mesenchymal-epithelial transition and its expression predicts liver and lymph node metastasis of CRC patients.** *PLoS ONE* 2012, *7*, e41335.

38. Li, X.; Xu, Y.; Chen, Y.; Chen, S.; Jia, X.; Sun, T.; Liu, Y.; Li, X.; Xiang, R.; Li, N. **SOX2 promotes tumor metastasis by stimulating epithelial-to-mesenchymal transition via regulation of WNT/β-catenin signal network.** *Cancer lett*. 2013, *336*, 379–389.

39. Cai, C.; Zhu, X. **The Wnt/β-catenin pathway regulates self-renewal of cancer stem-like cells in human gastric cancer.** *Mol. Med. Rep*. 2012, *5*, 1191–1196.

40. Takahashi, K.; Yamanaka, S. **Induction of pluripotent stem cells from mouse embryonic and adult fibroblast cultures by defined factors.** *Cell* 2006, *126*, 663–676.

41. Takahashi, K.; Tanabe, K.; Ohnuki, M.; Narita, M.; Ichisaka, T.; Tomoda, K.; Yamanaka, S. **Induction of pluripotent stem cells from adult human fibroblasts by defined factors.** *Cell* 2007, *131*, 861–872.

42. Wang, J.; Rao, S.; Chu, J.; Shen, X.; Levasseur, D.N.; Theunissen, T.W.; Orkin, S.H. **A protein interaction network for pluripotency of embryonic stem cells.** *Nature* 2006, *444*, 364–368.

43. Chen, S.; Xu, Y.; Chen, Y.; Li, X.; Mou, W.; Wang, L.; Liu, Y.; Reisfeld, R.A.; Xiang, R.; Lv, D.; et al. **SOX2 gene regulates the transcriptional network of oncogenes and**

affects tumorigenesis of human lung cancer cells. *PLoS ONE* 2012, *7*, e36326.

44. Arnold, S.J.; Stappert, J.; Bauer, A.; Kispert, A.; Herrmann, B.G.; Kemler, R. ***Brachyury* is a target gene of the Wnt/β-catenin signaling pathway.** *Mech. Dev*. 2000, *91*, 249–258.

45. Larocca, C.; Cohen, J.R.; Fernando, R.I.; Huang, B.; Hamilton, D.H.; Palena, C. **An autocrine loop between TGF-β1 and the transcription factor brachyury controls the transition of human carcinoma cells into a mesenchymal phenotype.** *Mol. Cancer Ther*. 2013, *12*, 1805–1815.

46. Hotta, K.; Takahashi, H.; Satoh, N.; Gojobori, T. **Brachyury-downstream gene sets in a chordate, Ciona intestinalis: Integrating notochord specification, morphogenesis and chordate evolution.** *Evol. Dev*. 2008, *10*, 37–51.

47. Ikushima, H.; Todo, T.; Ino, Y.; Takahashi, M.; Miyazawa, K.; Miyazono, K. **Autocrine TGF-β signaling maintains tumorigenicity of glioma-initiating cells through Sry-related HMG-box factors.** *Cell Stem Cell* 2009, *5*, 504–514.

48. Lou, X.; Han, X.; Jin, C.; Tian, W.; Yu, W.; Ding, D.; Cheng, L.; Huang, B.; Jiang, H.; Lin, B. **SOX2 targets fibronectin 1 to promote cell migration and invasion in ovarian cancer: New molecular leads for therapeutic intervention.** *Omics: A J. of Integr. Biol.* 2013, *17*, 510–518.

49. Hunt, G.C.; Singh, P.; Schwarzbauer, J.E. **Endogenous production of fibronectin is required for self-renewal of cultured mouse embryonic stem cells.** *Exp. Cell Res*. 2012, *318*, 1820–1831.

50. Gavert, N.; Vivanti, A.; Hazin, J.; Brabletz, T.; Ben-Ze'ev, A. **L1-mediated colon cancer cell metastasis does not require changes in EMT and cancer stem cell markers.** *Mol. Cancer Res*. 2011, *9*, 14–24.

51. Lou, Y.; Preobrazhenska, O.; auf dem Keller, U.; Sutcliffe, M.; Barclay, L.; McDonald, P.C.; Roskelley, C.; Overall, C.M.; Dedhar, S. **Epithelial-mesenchymal transition (EMT) is not sufficient for spontaneous murine breast cancer metastasis.** *Dev. Dyn.* 2008, *237*, 2755–2768.

52. Chikaishi, Y.; Uramoto, H.; Tanaka, F. **The EMT status in the primary tumor does not predict postoperative recurrence or disease-free survival in lung adenocarcinoma.** *Anticancer Res*. 2011, *31*, 4451–4456.

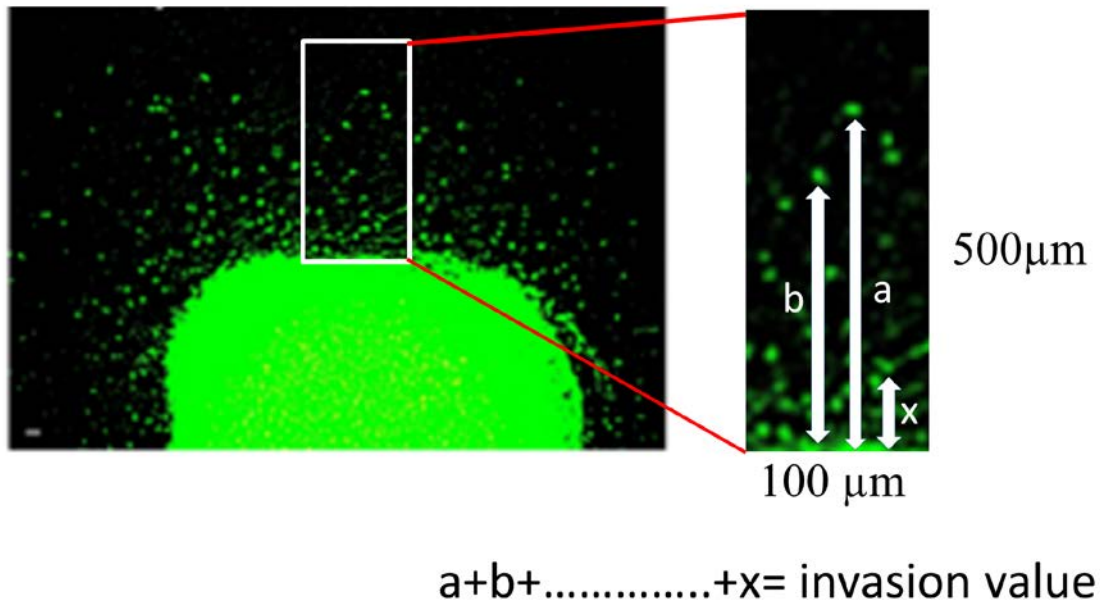

Supplemental Figure 1: Evaluation of Cancer cell invasiveness (Invasion Value).
Cancer cell invasiveness was evaluated by tumor dissemination from the tumor cell pellet (mimics a primary tumor nest). Evaluation were made by measuring the distance of all cells from the edge of the nest in 5 randomly selected standardised rectangular light fields (500 × 100 µm), and the values were summed.